Harmful Algae 98 (2020) 101896

Contents lists available at ScienceDirect

Harmful Algae

journal homepage: www.elsevier.com/locate/hal

Growth response of *Dinophysis, Mesodinium*, and *Teleaulax* cultures to temperature, irradiance, and salinity

James M. Fiorendino[a], Juliette L. Smith[b], Lisa Campbell[a,*]

[a] Department of Oceanography, Texas A&M University, College Station, TX 77843, USA
[b] Virginia Institute of Marine Science, College of William & Mary, Gloucester Point, Virginia, 23062, USA

ARTICLE INFO

Keywords:
Dinophysis
Mesodinium
Teleaulax
Harmful algal blooms
Diarrhetic shellfish poisoning
Okadaic Acid

ABSTRACT

Mixotrophic *Dinophysis* species threaten human health and coastal economies through the production of toxins which cause diarrhetic shellfish poisoning (DSP) in humans. Novel blooms of *Dinophysis acuminata* and *Dinophysis ovum* have occurred in North American waters in recent decades, resulting in the closure of shellfish harvesting. Understanding the ecology of *Dinophysis* species and their prey is essential to predicting and mitigating the impact of blooms of these dinoflagellates. The growth response of two new isolates of *Dinophysis* species, one isolate of *Mesodinium rubrum*, and two strains of *Teleaulax amphioxeia* were evaluated at a range of temperature, salinity, and irradiance treatments to identify possible environmental drivers of *Dinophysis* blooms in the Gulf of Mexico. Results showed optimal growth of *T. amphioxeia* and *M.* rubrum at 24 °C, salinity 30 – 34, and irradiances between 300 and 400 µmol quanta $m^{-2} s^{-1}$. Optimal *Dinophysis* growth was observed at salinity 22 and temperatures between 18 and 24 °C. *Mesodinium* and both *Dinophysis* responded differently to experimental treatments, which may be due to the suitability of prey and different handling of kleptochloroplasts. *Dinophysis* bloom onset may be initiated by warming surface waters between winter and spring in the Gulf of Mexico. Toxin profiles for these two North American isolates were distinct; *Dinophysis acuminata* produced okadaic acid, dinophysistoxin-1, and pectenotoxin-2 while *D. ovum* produced only okadaic acid. Toxin per cell for *D. ovum* was two orders of magnitude greater than *D. acuminata*. Phylogenies based on the *cox1* and *cob* genes did not distinguish these two *Dinophysis* species within the *D. acuminata* complex.

1. Introduction

Outbreaks of diarrhetic shellfish poisoning (DSP) are the result of toxin accumulation in the tissues of filter-feeding shellfish like mussels and oysters, specifically okadaic acid and the dinophysistoxins produced by species of marine dinoflagellates within the genus *Dinophysis* and some benthic species of *Prorocentrum* (Yasumoto et al., 1985; Pan et al., 1999; Ten-Hage et al., 2000). DSP is characterized by vomiting, diarrhea, and abdominal pain beginning shortly after consumption of contaminated shellfish and lasting several days (Yasumoto et al., 1978). In addition to gastrointestinal symptoms, toxins responsible for DSP have been shown to promote tumor growth in mice (Fujiki et al., 1988). Though usually not fatal, the prevalence of DSP events worldwide represents a considerable threat to not only human health, but coastal economies due to harvesting restrictions when toxin concentrations in shellfish exceed regulatory limits. Blooms of *Dinophysis* and associated DSP poisoning events are therefore a challenge for shellfish fisheries and aquaculture.

Dinophysis species are the main cause of DSP poisoning events around the world (Reguera et al., 2012). These dinoflagellates are found globally in coastal and oceanic waters of tropical and temperate regions, usually below 100 cells L^{-1} (Hallegraeff and Lucas, 1988). *Dinophysis* species are known to bloom seasonally and can grow to cell densities of 10^3 - 10^5 cells L^{-1} (Kat, 1983; Aubry et al., 2000; Reguera et al., 2012; Harred and Campbell, 2014). Blooms of toxigenic *Dinophysis* species are of particular concern because shellfish may accumulate enough toxins to become acutely toxic while *Dinophysis* cells are present at relatively low densities, around 200 cells L^{-1} (Yasumoto et al., 1985). The low threshold for acute toxicity of *Dinophysis* blooms makes prediction and rapid response essential for mitigating efforts.

North American waters have historically been free of problematic *Dinophysis* blooms and associated DSP poisoning events. As was the case in Norway, the history of *Dinophysis* blooms and DSP poisoning events in the United States is likely “old, but weakly documented” (Dahl et al., 1996). In Narragansett Bay, a two-year survey from July 1983 to September 1985 for *Dinophysis* and DSP toxins found only one positive

* Corresponding author: Lisa Campbell, TAMU 3146 Eller O&M Building, College Station, TX 77843.
E-mail address: lisacampbell@tamu.edu (L. Campbell).

https://doi.org/10.1016/j.hal.2020.101896
Received 9 April 2020; Received in revised form 21 August 2020; Accepted 21 August 2020
Available online 29 August 2020
1568-9883/

result of diarrhetic toxins in mussel tissue and observed cell abundances of *D. acuminata* never exceeded 2 cells mL^{-1} (Maranda and Shimizu, 1987). On the west coast, *Dinophysis* species are a common component of marine phytoplankton but have not historically been known to cause illness in humans (Jester et al., 2009).

In 2008, *Dinophysis ovum* bloomed in the Gulf of Mexico along the Texas coast, and since then blooms of *Dinophysis acuminata* have been documented in New York and Washington State in 2011 and 2012, respectively (Campbell et al., 2010; Hattenrath-Lehmann et al., 2013; Trainer et al., 2013). The bloom of *D. ovum* along the Texas coast resulted in the closure of shellfish harvesting and a recall of oysters, becoming the first instance of such a response to a bloom of *D. ovum* in the United States. During this bloom, *D. ovum* densities were over 2×10^5 cells L^{-1} (Campbell et al., 2010; Deeds et al., 2010). The increasing intensity of *Dinophysis* blooms in North American waters represents an emerging threat to human health and fisheries in the United States. Compounding the problem of intensifying *Dinophysis* blooms in North American waters is the high variability of inter- and intraspecific toxicity of *Dinophysis* species (Reguera et al., 2014).

Anticipation and early warning of *Dinophysis* blooms requires an understanding of the unique ecology of *Dinophysis* species and their prey. *Dinophysis* and their prey, the marine ciliate *Mesodinium rubrum*, are mixotrophic and kleptoplastidic (Park et al., 2006; Smith and Hansen, 2007; Stoecker et al., 2017). Mixotrophy is a common behavior among marine protists manifesting in a variety of forms, from obligate to facultative mixotrophy (Stoecker et al., 2017). Dinoflagellates in the genus *Dinophysis* and the ciliate *M. rubrum* can be placed in Type III.B as described by Stoecker et al. (2017), as all are marine protists that engage in kleptoplastidy. The cryptophyte *Teleaulax amphioxeia* is a Type II mixotroph (Stoecker et al., 2017), containing inherited plastids and obtaining most of its carbon from photosynthesis but capable of preying upon heterotrophic bacteria and *Synechococcus* (Yoo et al., 2017). The source of plastids in *Dinophysis* and *M. rubrum* are cryptophytes within the genera *Teleaulax, Plagioselmis*, and *Geminigera* (Park et al., 2006; Hansen et al., 2012; Kim et al., 2012; Myung et al., 2013; Kim et al., 2017). These plastids are sequestered by *Dinophysis* following consumption of *M. rubrum* cells. Though *Dinophysis* species and *M. rubrum* can survive extended periods without prey, they are obligate mixotrophs and must consume prey and sequester new chloroplasts for long-term survival (Park et al., 2006; Smith and Hansen, 2007; Kim et al., 2012). The intimate trophic relationships between *Dinophysis, M. rubrum*, and their cryptophyte source of plastids suggests bloom events of *Dinophysis* are, at least in part, dependent upon interactions between predator and prey populations.

Studying the development and decline of harmful algal blooms is difficult without persistent monitoring. Fortunately, an Imaging FlowCytobot (IFCB) has been deployed in the Aransas Pass inlet, Port Aransas, TX since 2007. The Aransas Pass inlet is 14 m deep and 120–180 m wide and connects the Gulf of Mexico to six shallow (1–3 m), well-mixed coastal bays (Ward, 1997). The IFCB deployed at Aransas Pass has captured several blooms of *D. ovum* and *Mesodinium* spp. in the Gulf of Mexico over the last decade, including the 2008 bloom of *D. ovum*. Analysis of IFCB image data found that *Mesodinium* spp. occurred from mid-September to May, at temperatures between 23 and 29 °C and salinities between 30 and 34, while blooms of *Dinophysis* occurred from the end of January to May at temperatures between 11 and 19 °C and salinities between 28 and 33 (Harred and Campbell, 2014). However, the relationship between *Mesodinium* abundance and *Dinophysis* blooms in the Gulf of Mexico was weak (Harred and Campbell, 2014). Additionally, physical concentration of cells (e.g. Hetland and Campbell, 2007) was determined to have little effect on *Dinophysis* bloom onset along the Texas coast because no relationship was found between wind-driven transport and abundance of *Dinophysis* cells (Harred and Campbell, 2014). *Dinophysis* cells did appear to originate offshore and were carried into coastal embayments on incoming tides (Campbell et al., 2010). These results suggest environmental conditions (temperature, salinity) may promote or discourage *Dinophysis* bloom formation in the Gulf of Mexico and that physical concentration and the abundance of suitable prey are not by themselves reliable indicators of a possible *Dinophysis* bloom.

Dinophysis blooms in other regions have been reported to occur within specific ranges of temperature and salinity (Aubry et al., 2000; Koike et al., 2007). The extent to which *Dinophysis, Mesodinium*, and *Teleaulax* can maintain high growth rates with respect to these factors is currently unknown. Understanding the response of each organism to a wide range of possible environmental conditions may reveal locations and times when blooms are likely to occur. Additionally, as a cosmopolitan genus with representative populations around the world, geographically distinct strains and species of *Dinophysis, Mesodinium*, and *Teleaulax* may respond differently to these factors and consequently bloom at different times of the year. Blooms of *D. ovum* occurred between the end of January and May in the Gulf of Mexico (Harred and Campbell, 2014), but blooms of *Dinophysis* in Washington and New York occurred during summer months (Hattenrath-Lehmann et al., 2013; Trainer et al., 2013).

Here, the growth responses of two newly isolated species of *Dinophysis* from the United States are compared with respect to a range of salinity, temperature, and light intensity treatments. Based on initial morphology these isolates were identified as *D. ovu*m, a subtropical species isolated from the Gulf of Mexico, and *D. acuminata*, a temperate species from Chesapeake Bay (Wolny et al., 2020). Morphologically, these two *Dinophysis* species can be differentiated, though no genetic differences were observed in the ITS and LSU genes of single-picked cells of *D. ovum* and *D. acuminata* (Wolny et al., 2020). To further differentiate these two cryptic species, other genes (*cox1* and *cob*) and toxin profiles were explored for both species. To better understand *Dinophysis* bloom dynamics with respect to the relationship between predators and prey, growth responses were also investigated for a temperate isolate of *M. rubrum* from Denmark and a temperate and subtropical strain of *T. amphioxeia* from the Gulf of Mexico and Denmark. As with *Dinophysis*, growth was evaluated over a range of temperature, salinity, and irradiance treatments. The results of this work will improve prediction and mitigation efforts for blooms of *Dinophysis* by revealing conditions during which blooms of these organisms are most likely to occur, with a focus on the Gulf of Mexico.

2. Methods

2.1. Isolation and culture maintenance

Two new single-cell isolates of *Dinophysis* species were established for this comparative study following methods described in

Table 1
Identification and isolation information of *Teleaulax, Mesodinium*, and *Dinophysis* cultures used in this study.

Strain	Species	Collection Site	Collection Date	Isolator
K-0434	*Teleaulax amphioxeia*	The Sound, Denmark	March 1990	D. Hill
GoMTA	*Teleaulax amphioxeia*	Port Aransas,Texas, USA	Summer 2015	Darren W. Henrichs
MBL-DK2009	*Mesodinium rubrum*	Helsingør Harbor, Denmark	2009	Per J. Hansen
DAVA01	*Dinophysis acuminata*	Chesapeake Bay, Virginia, USA	March 2017	Juliette L. Smith
DoSS3195	*Dinophysis ovum*	Surfside Beach, Texas, USA	March 2019	James M. Fiorendino

Wolny et al. (2020): *D. acuminata* (DAVA01) was collected from Nassawadox, Chesapeake Bay, VA in March 2017 and *D. ovum* (DoSS3195) was collected from Surfside Beach, Freeport, TX in March 2019 (Table 1). A new isolate of *T. amphioxeia* was also established from surface water collected from the Mission Aransas Shipping Channel in Port Aransas, TX in summer 2015. *Teleaulax amphioxeia* cells were picked into 96-well tissue culture plates filled with 0.2 μm filtered seawater from the Mission Aransas Shipping Channel. Clonal isolates were established by serial dilution following initial isolation of *T. amphioxeia*.

Stock cultures were maintained at 20 °C, 100 μmol quanta m^{-2} s^{-1} at a 14: 10 h light: dark cycle under cool white fluorescence in L1 medium (Guillard and Hargraves, 1993) prepared from 0.2 μm filtered seawater collected from the Flower Garden Banks National Marine Sanctuary (27.89°N, 93.81°W) in the Gulf of Mexico. Stock *Dinophysis* cultures were maintained at salinity 22 while stock *Teleaulax* and *M. rubrum* cultures were maintained at salinity 30. Light levels were determined using a handheld QSL2101 radiometer (Biospherical Instruments, Inc., San Diego, CA, USA). Cultures were transferred every two weeks into acid-washed 50 mL glass Kimax tubes filled with 40 mL of fresh L1 medium. *Mesodinium rubrum* and *Dinophysis* cultures were fed their respective prey item at a ratio of 1:10 predator:prey. Both species of *Dinophysis* were maintained on *M. rubrum* fed the Danish cryptophyte (K-0434). Prior to the experiments, cultures were acclimated stepwise to treatment conditions. Light levels were increased or decreased in 50 μmol quanta m^{-2} s^{-1} increments every two days. Temperature was increased or decreased at 1 °C increments every 2 days. Salinity was altered by increments of two at normal transfer intervals. Upon reaching each set of experimental conditions cultures were acclimated for a period of two weeks prior to experimental initiation.

2.2. Growth experiments

Two geographically distinct species of *Dinophysis, D. acuminata* (DAVA01) and *D. ovum* (DoSS3195), one species of *M. rubrum* (MBL-DK2009), and two geographically distinct strains of *T. amphioxeia* (K-0434 from Denmark and GoMTA from the Gulf of Mexico) (Table 1) were grown at a range of temperature (12, 18, 24, 27 °C), salinity (22, 26, 30, 34), and irradiance (50, 100, 200, 300, 400 μmol quanta m^{-2} s^{-1}) treatments to determine the growth response of each organism to variable environmental conditions. Treatments were chosen based on the observed daily decadal average temperature (13.5 - 30 °C) and salinity (28.7 – 37.5) ranges for the Mission Aransas Shipping Channel in Port Aransas, TX (Fig. 1, data from NOAA National Estuarine Research Reserve System (NERRS) station MARSCWQ) and temperature and salinity ranges observed by Harred and Campbell (2014) during

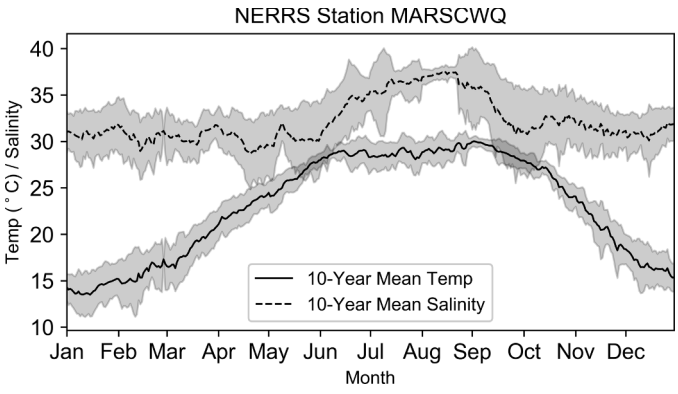

Fig. 1. Daily decadal average temperature and salinity at 5 – 7 m in the Mission Aransas Shipping Channel in Port Aransas, TX. Shaded regions represent one standard deviation about the mean. Data downloaded from the National Estuarine Research Reserve System for the Mission Aransas Shipping Channel Water Quality Station (MARSCWQ).

blooms of *Mesodinium* and *Dinophysis* species in the Gulf of Mexico. Attempts were made to acclimate DAVA01, DoSS3195, and *M. rubrum* to 30 °C, but cultures did not survive and so these treatments were not included in this study. *Dinophysis* cultures could not be maintained at 27 °C, either, so growth rates of DAVA01 and DoSS3195 were assumed to be zero at this temperature in statistical analyses.

Growth experiments were conducted in a full-factorial design for the range of temperature, irradiance, and salinity conditions described, with the exception of irradiance for *Dinophysis* species. Irradiances above 100 μmol quanta m^{-2} s^{-1} were found not to further impact growth of either DAVA01 or DoSS3195, so additional experimental treatments at 200, 300, and 400 μmol quanta m^{-2} s^{-1} were discontinued for this genus. For *M. rubrum* and *Dinophysis*, experiments began with cell counts of parent cultures from which cell densities were calculated. Counts were performed by gently swirling cultures prior to taking 2 mL aliquots from parent cultures. Aliquots were subsequently fixed with a 5% Lugol's iodine solution (LabChem Inc., Zelienople, PA, USA) and used to fill Sedgewick-Rafter counting chambers. Cells were enumerated via light microscopy on an Olympus BX60 microscope (Olympus Corporation, Shinjuku City, Tokyo, Japan). One slide was counted per culture and a minimum of 200 cells were counted per slide. For *Teleaulax*, cell densities were determined with a TD 700 fluorometer (Turner Designs, Inc., San Jose, CA, USA). Densities of cells were calibrated to fluorescence readings based on manual counts of a dilution series prepared from a parent *Teleaulax* culture. Independent calibrations were performed for both K-0434 and GoMTA strains.

Once the cell densities of parent cultures were determined, cultures were transferred into fresh L1 media at desired inoculation densities, usually 300 cells mL^{-1} for *Mesodinium* and *Dinophysis* and 3000 cells mL^{-1} for *Teleaulax*. Both *M. rubrum* and *Dinophysis* were given prey at the predator:prey ratio described for stock cultures in Section 2.1. Over the course of the growth period, cultures were enumerated at intervals of between 1 and 4 days, depending upon the experimental treatment. Experiments were conducted between one and three weeks. Neither *Mesodinium* nor *Dinophysis* were diluted or provided additional prey during experiments. *Mesodinium rubrum* and *Dinophysis* were enumerated via light microscopy and *Teleaulax* via fluorometry over the course of the experiment. Once cultures were determined to be growing exponentially, growth rates (μ, d^{-1}) were calculated using the equation (Guillard, 1973):

$$\mu = \frac{ln\left(\frac{N}{N_0}\right)}{t - t_0}$$

where N is the cell density of an experimental culture at time t, and N_0 is the initial cell density at the beginning of the exponential growth phase t_0; $t - t_0$ is the time elapsed between cell counts. $t - t_0$ used in growth rate calculations spanned at least three data points during the exponential growth phase. Examples of growth curves for *Dinophysis, Mesodinium*, and *Teleaulax*, including selected points for growth rate calculations, are shown in Fig. 2.

2.3. Toxin analysis

Extracellular and intracellular toxins were extracted from cultures of DAVA01 and DoSS3195 during exponential growth under maintenance conditions: 15 °C, 100 μmol quanta m^{-2} s^{-1}. Medium (3 mL) was separated from cells (6000) using centrifugation: 15 min at 3500 *x g* at 4 °C. The medium was immediately extracted for extracellular toxins and subjected to clean-up using solid phase extraction: HLB 3 cc, 60 mg (Oasis, Waters Corp., Milford, MA, USA), using methods previously described in Smith et al. (2018). The original cell pellet was immediately bath sonified with 0.5 mL of 100% methanol for 15 min at 25 Hz, and centrifuged for 15 min at 3500 *x g*. The supernatant was spin filtered (0.2-μm nanosep) for 30 s at 3500 *x g*, and the filtrate stored at −20 °C until analysis of intracellular toxins.

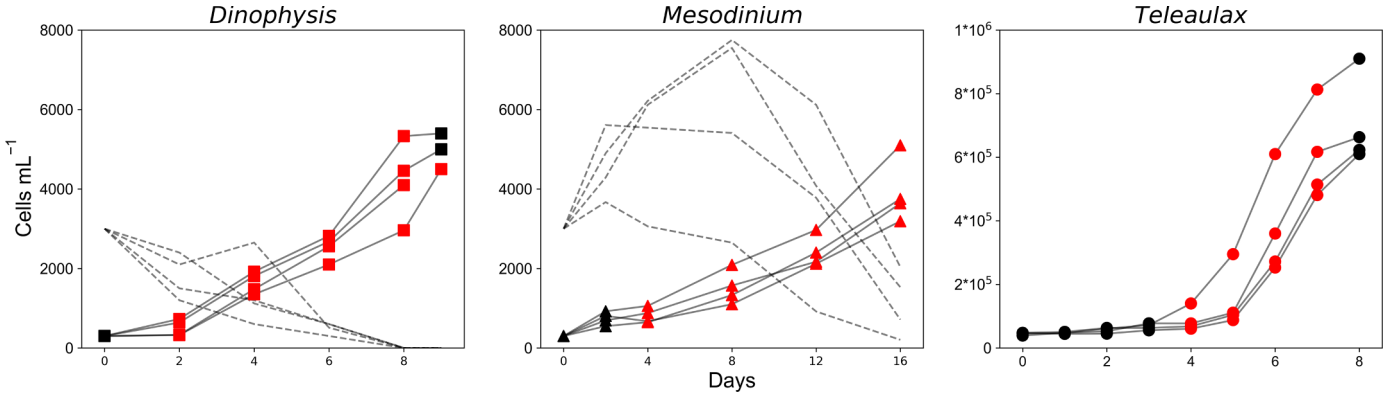

Fig. 2. Growth curves for *Dinophysis, Mesodinium*, and *Teleaulax*. Red points were used for growth rate calculations. Black points were excluded from growth rate calculations. The dotted lines in the *Dinophysis* and *Mesodinium* panels represent prey abundance.

Detection and quantification of toxins was conducted using ultra performance liquid chromatography (Acquity, Waters Corp., Milford, MA, USA) coupled to tandem mass spectrometry, UPLC-MS/MS (Xevo MS, Waters Corp., Milford, MA, USA) with a trapping dimension and at-column dilution (Onofrio et al., 2020). Reference standards were purchased from National Research Council, Halifax, Canada: dinophysis-toxin-1 (DTX1, CRM-DTX1-b), dinophysistoxin-2 (DTX2, CRM-DTX2-b), okadaic acid (OA, CRM-OA-d), pectenotoxin-2, (PTX2, CRM-PTX2-b). Quantification was done using MRM transitions: DTX1 *m/z* 817.5 > 113.0; DTX2 *m/z* 803.5 > 255.5; OA *m/z* 803.5 > 255.5; PTX2 *m/z* 876.6 > 841.5. The first three toxins were detected in ESI- mode, while PTX2 was run in ESI+. Cone voltage was 30 V, and collision energy was 30 eV for PTX2 and ranged from 60 to 70 eV, depending on the DSP toxin. Triple standard curves were run; curves ranged from 0.5 µg/L to 50 µg/L using a 50-µL injection volume.

2.4. Phylogeny and species identification

DNA was extracted from *Teleaulax* and *Dinophysis* species following the cetyltrimethylammonium bromide extraction protocol (Rogers and Bendich, 1994). Cultures were pelleted prior to DNA extraction, and cells broken by centrifugation with glass beads. Cultures of *Dinophysis* were only pelleted once complete consumption of *M. rubrum* prey had been visually confirmed. The mitochondrial *cox1* (primers: DinoCOX1F and DinoCOX1R from Lin et al., 2002) and *cob* (primers: Dinocob1F and Dinocob1R from Zhang et al., 2005) regions of *Dinophysis* DNA were amplified. For *Teleaulax* the LSU (D1/D2; primers: D1R and D2C from Scholin et al., 1994) and 18S (primers: 18SA and 18SB from Medlin et al., 1988) regions were amplified. All PCR reactions were performed in a 50 µL reaction containing ca. 10 ng of extracted genomic DNA, 0.5 µM primers and 1x GoTaq® Green Master Mix (Promega, Madison, WI, USA). Thermocycler parameters were set at initial denaturation 95 °C for 300 s, followed by 40 cycles of denaturation at 95 °C for 30 s, annealing at 54 °C for 60 s, extension at 72 °C for 90 s, with a final extension step of 15 min at 72 °C. All PCR were performed with a negative control. PCR-generated products were visualized on a 1.5% agarose gel under UV and purified using a Qiagen DNA Gel clean up kit (Qiagen, Hilden, Germany). PCR products were Sanger sequenced at the Institute for Plant Genomics and Biotechnology at Texas A&M University (498 Olsen Blvd, College Station, TX, USA). Forward and reverse sequences were combined into contigs and aligned using BioEdit v7.2 (Hall, 1999). Any site showing an ambiguity in the forward and reverse sequences was recorded as such. Sequences were aligned in SeaView v4.6.1 (Gouy et al., 2010) using Clustal Omega (Sievers et al., 2011) with additional sequences downloaded from Genbank.

Maximum likelihood (ML) trees were inferred using the RAxML tool as implemented in RAxMLGUI v2.0 beta (Silvestro and Michalak, 2012; Stamatakis, 2014; Edler et al., 2019) using a heuristic search (ten random additions of sequences run), rapid hill climbing mode (default), TBR branch swapping, and a GTRGAMMA base substitution model. Bootstrap values were obtained with 1000 bootstrap replicates and one random addition of sequences run per bootstrap replicate (thorough bootstrap analysis). Generated trees were visualized using MEGA X v10.0.5 (Kumar et al., 2018). Differences between sequences were calculated using MEGA X v10.0.5, as well (Tamura et al., 2013). Sequences generated in this study were submitted to GenBank under the accession numbers: MT299237: GoMTA 18S, MT299238: K-0434 18S, MT299239: GoMTA 28S, MT299240: K-0434 28S, MT309108: DAVA01 *cox1*, MT309109: DoSS3195 *cox1*, MT309110: DoSS3195 *cob*, MT309111: DAVA01 *cob*.

2.5. Statistical analyses

Individual and interactive effects on growth with regard to temperature, salinity, and irradiance were tested by three and four-way ANOVA. Four-way ANOVA was used when testing for differences between strains of *Teleaulax* and between species of *Dinophysis*. If significant effects were found, differences in growth between individual treatments or between strains and species were tested for statistical significance by t-tests. Homogeneity of growth rate variance was determined by Levene's test (Levene, 1960). When variances were unequal, Welch's *t*-test (Welch, 1947) was used instead of a standard *t*-test. A correction of p-values was performed according to the method described by Benjamini and Hochberg (1995) to account for rare events due to the large number of treatments being compared. Data analysis, t-tests, and Levene's tests were performed in Python v3.5.5 (van Rossum and Drake, 2011) using the SciPy package v1.1.0 (Virtanen et al., 2020) and the Pandas package v0.23.4 (McKinney, 2010). ANOVA tests were performed in R v3.5.3 (R Core Team, 2019). To determine which factors most impacted growth rates of *Teleaulax, Mesodinium*, and *Dinophysis*, ω^2 values (Olejnik and Algina, 2003) were calculated for each individual factor and combination of factors using the R package sjstats v0.17.9 (Lüdecke, 2020).

3. Results

Raw cell count data for all experiments are available in supplementary materials (Supplementary Tables S1 – S8). A python script (GROWTH_CURVE_PLOTTER.py) to easily visualize growth curves is included, as well.

3.1. Teleaulax

A representative culture of *T. amphioxeia* (GoMTA, Table 1) was established from the Gulf of Mexico. The GoMTA strain of *T. amphioxeia* grew over the full range of experimental treatments (Fig. 3, Row A).

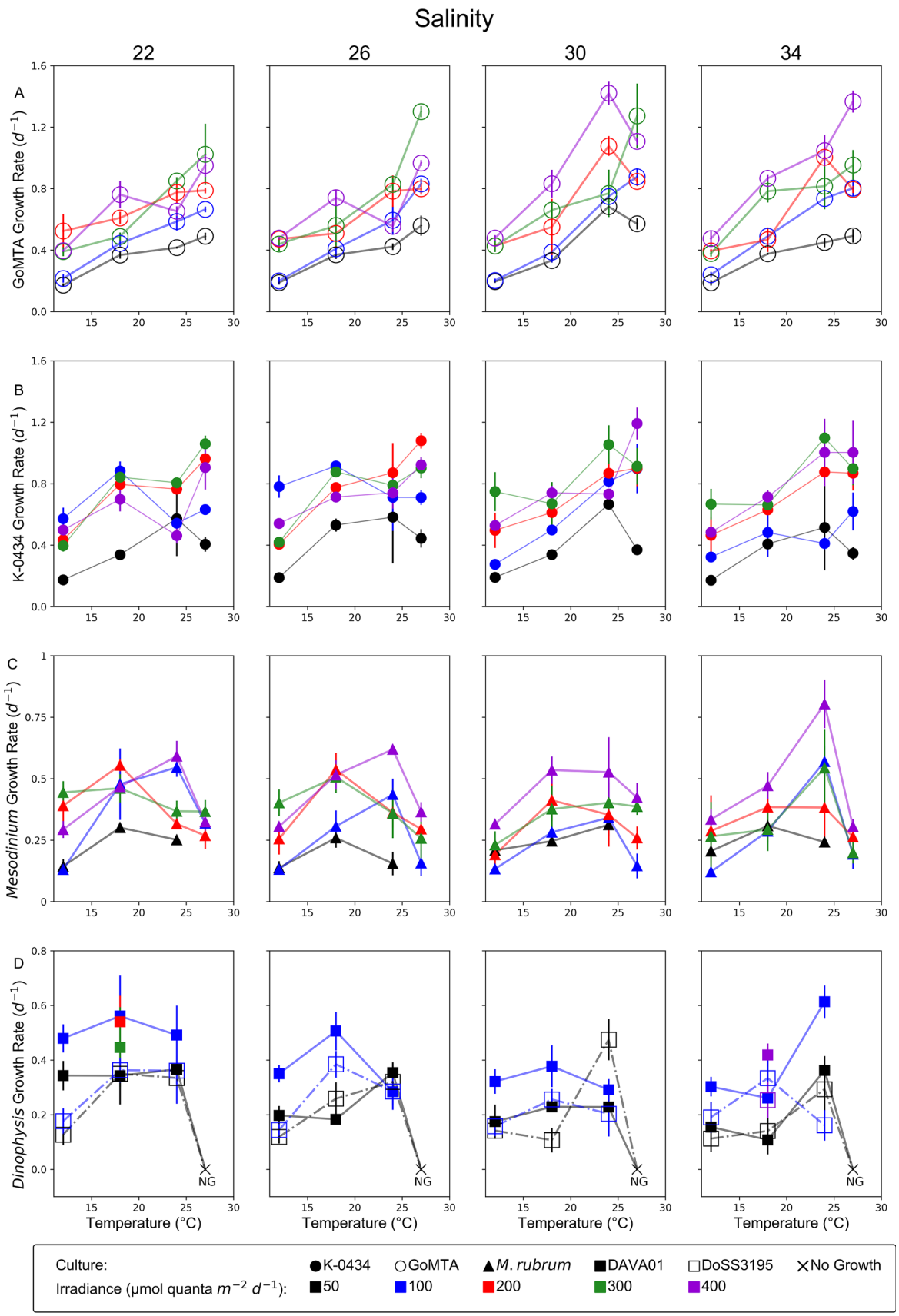

Fig. 3. Growth rates (d^{-1}) of *Teleaulax* (K-0434 and GoMTA), *Mesodinium rubrum* (MBL-DK2009), and *Dinophysis* (DAVA01 and DoSS3195) species. Growth rates (y axes) in each panel are plotted against temperature (x axes). Color represents irradiance (Black = 50, Blue = 100, Red = 200, Green = 300, Purple = 400 µmol quanta m^{-2} s^{-1}). From left to right, columns represent salinity 22, 26, 30, and 34. Rows A, B, C, and D show growth rates of GoMTA, K-0434, *M. rubrum*, and both species of *Dinophysis*, respectively.

Maximum mean growth rate of GoMTA, 1.42 +/- 0.07 d^{-1}, was observed at 24 °C, 400 µmol quanta $m^{-2} s^{-1}$, salinity 30. Minimum growth, 0.17 +/- 0.01 d^{-1}, was observed at 12 °C, 50 µmol quanta $m^{-2} s^{-1}$, salinity 22. Results of the three-way ANOVA showed a significant growth response to temperature, salinity, and irradiance independently, as well as interactions between variables ($p < 0.0001$; Supplementary Table S9). Temperature and irradiance accounted for the largest proportion of growth variance ($\omega^2 = 0.48$, 0.27 respectively; Supplementary Table S9), together accounting for ~75% of growth rate variability. Growth rates of GoMTA increased with increasing temperature and irradiance. Growth rates at the highest irradiance treatment (400 µmol quanta $m^{-2} s^{-1}$) were often the highest observed for specific temperature and salinity treatments. GoMTA growth was minimally affected by salinity, but results suggest GoMTA is capable of higher maximum growth rates at salinities of 30 and above. At salinity 22, GoMTA was never observed to grow at a rate of 1.2 d^{-1} or above, which occurred at least once at salinities of 26 and above.

The Danish strain of *Teleaulax*, K-0434 (Fig. 3, Row B), was also capable of growing well over the full range of treatments, showing similar growth trends to those observed for GoMTA. K-0434 grew fastest at 27 °C, 400 µmol quanta $m^{-2} s^{-1}$, and salinity 30 at 1.19 +/- 0.1 d^{-1} and grew slowest at 12 °C, 50 µmol quanta $m^{-2} s^{-1}$, and salinity 34 at a rate of 0.17 +/- 0.02 d^{-1}. Maximal growth fell within the temperature (23 – 29 °C) and salinity (30 – 34) range observed for blooms of *Mesodinium*, but outside the temperature (11 – 19 °C) range for observed *Dinophysis* blooms (Harred and Campbell, 2014). Growth rates increased between 12 and 24 °C, where growth began to plateau.

Three-way ANOVA results showed significant effects on growth for salinity, temperature, and irradiance independently as well as significant interacting effects between these three factors ($p < 0.0001$; Supplementary Table S9). Temperature and irradiance again accounted for the highest proportions of growth variability ($\omega^2 = 0.32$, 0.28 respectively; Supplementary Table S9). Growth of K-0434 peaked at lower light levels when grown at lower salinity and temperature. At 18 °C and below and salinity 22 and 26 (Fig. 3, Row B), maximum growth was achieved at 100 µmol quanta $m^{-2} s^{-1}$. Above this irradiance, growth did not increase except at temperatures above 18 °C, where maximum growth occurred at 200 µmol quanta $m^{-2} s^{-1}$. At higher salinities (30 – 34), K-0434 achieved maximum growth between 300 and 400 µmol quanta $m^{-2} s^{-1}$.

Results of four-way ANOVA indicated the two strains of *T. amphioxeia* responded differently to the range of conditions tested ($p < 0.0001$; Supplementary Table S9). Again, temperature and irradiance accounted for the greatest percentage of variance in *Teleaulax* growth ($\omega^2 = 0.38$, 0.26 respectively; Supplementary Table S9). Overall, the effect of strain identity on *T. amphioxeia* growth was minimal ($\omega^2 = 0.004 – 0.03$, Supplementary Table S9), and the two strains of *T. amphioxeia* tested showed similar trends in growth with regard to temperature. Specifically, *T. amphioxeia* growth rates increased with increasing temperature up to 24 °C. The GoMTA strain did not respond to irradiance at low salinities and temperatures in the same way as the K-0434 strain, that is, with suppression of or no increase in growth rate above 100 µmol quanta $m^{-2} s^{-1}$. GoMTA growth rates increased up to at least 200 µmol quanta $m^{-2} s^{-1}$ at low temperature and salinity before beginning to plateau. It is at low salinity and temperature where growth of these two strains are most often significantly different (Supplementary Table S10). Additionally, K-0434 growth rates were saturated with respect to irradiance above 300 µmol quanta $m^{-2} s^{-1}$ while GoMTA, particularly at higher salinities and temperatures, often grew fastest at 400 µmol quanta $m^{-2} s^{-1}$.

3.2. Mesodinium

Mesodinium rubrum grew at nearly every experimental treatment. At 27 °C, 50 µmol quanta $m^{-2} s^{-1}$, *M. rubrum* was overgrown by its prey, *T. amphioxeia*, and no stable culture could be maintained. Growth of *M. rubrum* (Fig. 3, Row C) was highest at 24 °C, 400 µmol quanta $m^{-2} s^{-1}$, and salinity 34 at 0.8 +/- 0.1 d^{-1}. Slowest growth was observed at 12 °C, 100 µmol quanta $m^{-2} s^{-1}$, and salinity 34 at 0.12 +/- 0.02 d^{-1}. Growth rates of *M. rubrum* plateaued between 18 and 24 °C, above which growth began to decline. At 27 °C, growth rates of *M. rubrum* fell sharply and the ciliate struggled to clear tubes of cryptophyte prey. At 100 µmol quanta $m^{-2} s^{-1}$, *M. rubrum* was overgrown by *T. amphioxeia* during the growth experiment. No experiment could be run below 100 µmol quanta $m^{-2} s^{-1}$ because stock cultures were continuously overgrown by *T. amphioxeia*. Results of three-way ANOVA show a significant ($p < 0.01$; Supplementary Table S9) growth response of *M. rubrum* to each of the factors tested, as well as significant interacting effects on growth between temperature, irradiance, and salinity. Temperature and irradiance accounted for the largest proportion of variance of *M. rubrum* growth ($\omega^2 = 0.26$, 0.22 respectively; Supplementary Table S9). Though the impact of salinity on growth of *M. rubrum* was small ($\omega^2 = 0.01$, Supplementary Table S9), there is an apparent shift in the growth response of *M. rubrum* to temperature at different salinities. At low salinities (22 and 26), *M. rubrum* growth begins to plateau at ~18 °C. At salinity 34, growth rates increased steadily up to 24 °C before sharply falling at 27 °C. It is at salinity 34 where the maximum growth rates were achieved, as well.

3.3. Dinophysis

The *D. acuminata* isolate DAVA01 grew at the full range of salinities (22 – 34), temperatures (12 – 24 °C), and irradiances (50 and 100 µmol quanta $m^{-2} s^{-1}$) tested (Fig. 3, Row D). Experiments at irradiances above 100 µmol quanta $m^{-2} s^{-1}$ were discontinued, because high light did not result in significantly different growth at 18 °C in early trials ($p > 0.05$; Supplementary Figure S1). At 18 °C, 100 µmol quanta $m^{-2} s^{-1}$, and salinity 22 mean growth rate of DAVA01 was 0.56 +/- 0.15 d^{-1}. At the same salinity and temperature but 200 and 300 µmol quanta $m^{-2} s^{-1}$, mean growth rate of DAVA01 was 0.54 +/- 0.1 d^{-1} and 0.45 +/- 0.15 d^{-1}, respectively. At 18 °C and salinity 34, acclimation to 400 µmol quanta $m^{-2} s^{-1}$ did increase the mean growth rate of DAVA01 significantly ($p < 0.05$; Supplementary Figure S1) relative to the observed mean growth rate at 100 µmol quanta $m^{-2} s^{-1}$, from 0.26 +/- 0.09 d^{-1} to 0.42 +/- 0.04 d^{-1}. The increased growth rate observed was still less than those observed for the same temperature treatment at lower salinities and irradiance, however. Growth rate of DAVA01 was highest at 24 °C, 100 µmol quanta $m^{-2} s^{-1}$, and salinity 34 at a rate of 0.61 +/- 0.06 d^{-1}. Growth of DAVA01 was slowest at 18 °C, 50 µmol quanta $m^{-2} s^{-1}$, and salinity 34 at a rate of 0.11 +/- 0.05 d^{-1}. At salinity 22, DAVA01 growth was consistent between 12 and 24 °C and was fastest at 100 µmol quanta $m^{-2} s^{-1}$ within this range of temperatures. Above 24 °C growth decreased, and DAVA01 cultures did not grow in attempts to acclimate to 27 °C. This trend of consistent growth rates between 12 and 24 °C was also apparent at salinities of 26 and 30, though growth rates appeared to generally decrease with increasing salinity. At the highest salinity tested (34), there was a steep increase in growth at 24 °C at both 100 and 50 µmol quanta $m^{-2} s^{-1}$ before growth rate again fell at temperatures exceeding 24 °C.

Results of three-way ANOVA for DAVA01 growth rates showed significant ($p < 0.01$; Supplementary Table S9) growth responses to salinity, temperature, and irradiance independently, as well as significant interactions between temperature and irradiance, and temperature, irradiance, and salinity. Interactive effects of salinity and irradiance were not significant ($p > 0.05$). Salinity, temperature, and irradiance accounted for comparable proportions of DAVA01 growth rate variance ($\omega^2 = 0.24$, 0.19, 0.21 respectively; Supplementary Table S9).

A *D. ovum* isolate (DoSS3195, Table 1) was established successfully from the Gulf of Mexico. DoSS3195 (Fig. 3, Row D) was grown under similar treatments to DAVA01, and again high light treatments were

excluded. The single high-light treatment (18 °C, 400 μmol quanta $m^{-2} s^{-1}$, salinity 34) produced a mean growth rate not statistically different ($p > 0.05$; Supplementary Figure S2) from the mean growth rate observed at 100 μmol quanta $m^{-2} s^{-1}$ for salinity 34 and 18 °C: 0.33 +/- 0.08 d^{-1} at 100 μmol quanta $m^{-2} s^{-1}$ and 0.25 +/- 0.07 d^{-1} at 400 μmol $m^{-2} s^{-1}$. Highest growth rate of DoSS3195 was observed at 24 °C, 50 μmol quanta $m^{-2} s^{-1}$, and salinity 30 at 0.47 +/- 0.08 d^{-1}. Slowest growth was observed at 12 °C, 50 μmol quanta $m^{-2} s^{-1}$, salinity 34 at 0.11 +/- 0.002 d^{-1}. Optimal growth for DoSS3195 was observed at temperatures between 18 and 24 °C. Outside of this range, growth rates were suppressed and temperatures above 24 °C resulted in mortality of DoSS3195. Generally, DoSS3195 grew maximally at 50 μmol quanta $m^{-2} s^{-1}$. In most cases growth rates at higher irradiances (above 50 μmol quanta $m^{-2} s^{-1}$) were not significantly different than growth rates observed at 50 μmol quanta $m^{-2} s^{-1}$ ($p > 0.05$; Supplementary Figure S2).

Results of the three-way ANOVA for DoSS3195 showed significant ($p < 0.05$, Supplementary Table S9) responses of growth rate to salinity and temperature independently and to the interacting effects of salinity, temperature, and irradiance. The effect of irradiance alone on DoSS3195 growth was not significant ($p > 0.05$, Supplementary Table S9). Temperature and temperature x irradiance interactions had the largest effect on DoSS3195 growth variability ($\omega^2 = 0.47$, 0.14 respectively; Supplementary Table S9), with temperature alone accounting for nearly half of the observed growth rate variability.

Results of four-way ANOVA for *Dinophysis* species showed a significant difference in growth response to experimental factors between species ($p < 0.0001$, Supplementary Table S9). DoSS3195 growth rate was more sensitive to temperature than DAVA01. At 12 °C DoSS3195 growth rate (~0.15 d^{-1}) was suppressed relative to growth between 18 and 24 °C (~0.35 d^{-1}). In contrast, DAVA01 mean growth rates did not change significantly between 12 and 18 °C (Supplementary Figure S1) and were significantly ($p < 0.05$) greater than DoSS3195 growth rates at 50 and 100 μmol quanta $m^{-2} s^{-1}$ when grown at salinity 22 and 26 (Supplementary Table S10). Both species shared a sensitivity to temperatures above 24 °C. Growth rates of DAVA01 and DoSS3195 fell rapidly above 24 °C and neither could be maintained at 27 °C. DoSS3195 also exhibited a steep increase in growth rate at 24 °C, salinity 30 similar to the growth rate spike observed for DAVA01 at 24 °C and salinity 34. This spike only occurred at 50 μmol quanta $m^{-2} s^{-1}$ for DoSS3195, while it occurred at both 50 and 100 μmol quanta $m^{-2} s^{-1}$ for DAVA01. As with DAVA01, this peak represented the maximum growth rate of DoSS3195. Consistent growth was observed between 18 and 24 °C and salinity 22 and 26 for both isolates.

3.4. Toxin profiles

A disparity in toxin profile between DAVA01 and DoSS3195 was observed, with the *D. acuminata* isolate DAVA01 containing intracellular OA, DTX1, and PTX2 (Fig. 4). *Dinophysis ovum* (DoSS3195), however, only contained intracellular OA at detectable levels. A simpler profile was observed in the extracellular fraction of the DAVA01 isolate, with only the most abundant toxin, PTX2, detected in the medium. The extracellular profile for the DoSS3195 isolate matched the intracellular profile, with only OA detected (Table 2). Once values were standardized through conversion to the amount of toxin per cell, it was apparent that levels in the medium (extracellular) were lower than those detected in the cells (intracellular) at the point of harvesting, i.e., exponential growth (Table 2). By comparing between species, DoSS3195 contained almost two orders of magnitude more intracellular OA per cell (62.3 pg/cell) than DAVA01 (0.7 pg/cell). This pattern held even when OA and DTX1 values were summed to represent total intracellular DSP toxin content in DAVA01 (0.8 pg/cell). The DSP toxin DTX2 was not detected in either culture.

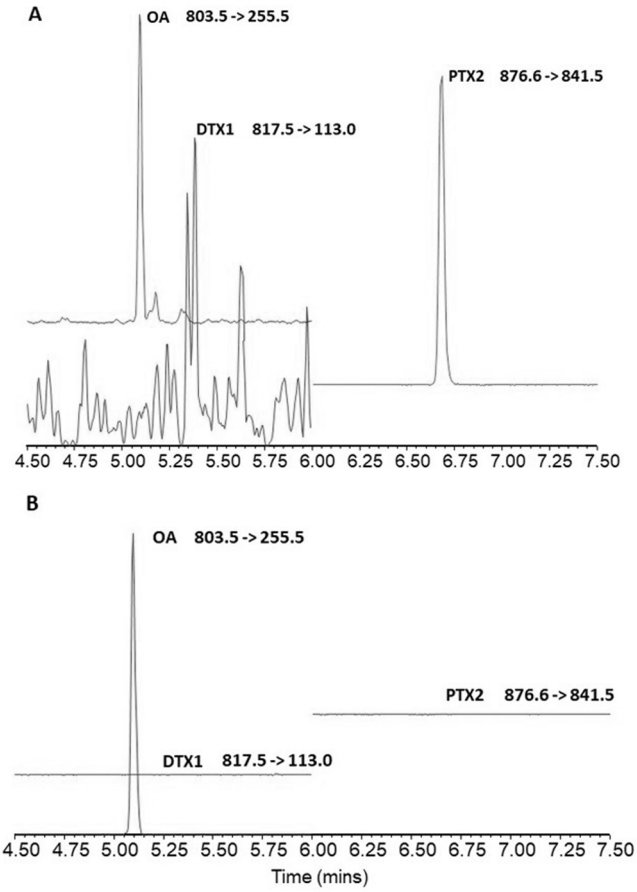

Fig. 4. Chromatograms for intracellular OA, DTX1, and PTX2 in *Dinophysis* spp. isolates DAVA01 (A) and DoSS3195 (B) using LC-MS/MS.

3.5. Phylogenies

Phylogenies inferred from the ML analysis of *cob* and *cox1* genes for *Dinophysis* isolates showed that all *Dinophysis* species are monophyletic, grouped into a common clade with high bootstrap support (Supplementary Figure S3). Based on the ML analysis using the *cob* gene, the two new isolates of *D. acuminata* (DAVA01) and *D. ovum* (DoSS3195) resolved in a single clade with other species of *Dinophysis* (Supplementary Figure S3A). Three clades of *Dinophysis* were resolved in phylogenies inferred from the *cox1* gene (Supplementary Figure S3B). *Dinophysis acuta* formed a single clade with 81% support. Of the other two sister clades, one clade contained *cox1* sequences from *Dinophysis tripos* and *Dinophysis miles* (61%) and the other clade (64%) contained *Dinophysis* species belonging to the *D. acuminata* species complex (*D. acuminata, Dinophysis sacculus, D. ovum*). DAVA01 and DoSS31195 *cox1* sequences fell within the *D. acuminata* complex. In both trees, ramification was apparent in the *D. acuminata* complex and ingroups formed clades with weak bootstrap support (64% in both phylogenies).

Phylogenetic trees inferred from ML analysis of cryptophyte 18S sequences grouped GoMTA and K-0434 with other sequences of *T. amphioxeia* (Supplementary Figure S4). The 18S sequences for K-0434 were nearly identical to other representative sequences of *T. amphioxeia* (Supplementary Figure S4A). Estimated distances between the GoMTA 18S sequence and other *T. amphioxeia* 18S sequences were between 0.003 and 0.0037, corresponding to a 5–6 nucleotide difference in a ~1630 base pair alignment. Distances between K-0434 18S sequences and other *T. amphioxeia* 18S sequences, excluding GoMTA, were

Table 2
Cellular content (toxin/cell) and concentrations (toxin/mL) of DTX1, OA, and PTX2 in the methanolic extract from the intracellular and extracellular fractions of the DoSS3195 and DAVA01 cultures during exponential growth.*Dinophysis ovum* (DoSS3195) and *D. acuminata* (DAVA01) DTX2 was also analyzed, but was not detected in the monocultures.

Isolate	OA			DTX1			PTX2		
	Intra Content (pg/cell)	Extra Content (pg/cell)	Conc. (ng/mL)	Intra Content (pg/cell)	Extra Content (pg/cell)	Conc. (ng/mL)	Intra Content (pg/cell)	Extra Content (pg/cell)	Conc. (ng/mL)
DoSS3195	62.3	4.1	1.0	–	–	–	–	–	–
DAVA01	0.7	–	–	0.1	–	–	54.8	2.4	1.4

Conc. = concentration, Intra = intracellular, Extra = extracellular, "—" = non-detect and/or below detection limit.

between 0.00 and 0.0006, corresponding to 0–1 differences in nucleotides in a ~1630 nucleotide alignment. LSU sequences of GoMTA and K-0434 also formed a clade with a third *T. amphioxeia* LSU sequence from Genbank (Supplementary Figure S4B).

4. Discussion

4.1. Physiological response to temperature, salinity, and irradiance

The primary factors influencing *T. amphioxeia* growth were irradiance and temperature, consistent with a primarily phototrophic lifestyle. The cryptophyte *T. amphioxeia* has recently been shown to be capable of feeding on the cyanobacterium *Synechococcus* and heterotrophic bacteria, though predation accounts for only 6–7% of total *T. amphioxeia* cellular carbon (Yoo et al., 2017). *Teleaulax amphioxeia* is, therefore, primarily photosynthetic. Cultures used in these experiments were non-axenic, so *T. amphioxeia* would have been able to consume bacteria present in culture medium. Observed growth rates were possibly a better representation of *in-situ* growth rates than axenic cultures would have been. The small amount of carbon that may have been attained by *T. amphioxeia* from predation on bacteria was likely supplemental and did not offset any decreases in photosynthetic efficiency resulting from unfavorable temperature or irradiance, as indicated by the relationship between *T. amphioxeia* growth rate and temperature and irradiance. Future experiments investigating the importance of grazing with regard to *T. amphioxeia* growth will be informative from a physiological and ecological perspective.

Both strains of the cryptophyte *T. amphioxeia* were capable of sustaining growth over a wide range of temperature, salinity, and irradiance conditions, and both revealed maximum growth rates at similar ranges of temperature and salinity (24 °C, salinity 30 – 34). However, the response to irradiance of these two cryptophyte strains differed at the lower salinities (22 – 26) and temperatures (12 – 18 °C) tested. Beyond suppressed growth rates at lower temperatures, K-0434 growth plateaued at lower irradiance than GoMTA at the same temperature treatments. Maximum growth rates were achieved at 100 µmol quanta $m^{-2} s^{-1}$ for K-0434 at 12 and 18 °C, and at irradiances above 100 µmol quanta $m^{-2} s^{-1}$ at warmer temperatures. GoMTA growth was maximal at 200 – 400 µmol quanta $m^{-2} s^{-1}$ at 12 and 18 °C. Temperature is known to induce photoacclimation in algae (Maxwell et al., 1994). The strain K-0434, which was isolated from higher latitude waters, may be less able to cope with high irradiance at lower temperatures than the GoMTA strain, which was isolated from a subtropical region receiving greater insolation. At lower temperature, K-0434 photosystems may be damaged by irradiances above 100 µmol quanta $m^{-2} s^{-1}$.

Previous studies have shown both *M. rubrum* and *Dinophysis* species, though capable of surviving for days to weeks without prey, must consume prey for long-term survival (Park et al., 2006; Smith and Hansen, 2007). *Dinophysis acuminata* can consume between 3 and 9 *M. rubrum* per day, accounting for up to 90% of gross carbon intake (Kim et al., 2008; Riisgaard and Hansen, 2009). *Mesodinium rubrum* can consume up to 6 *T. amphioxeia* per day, accounting for up to 22% of gross carbon uptake, but can maintain maximum growth rates on ~1 *T. amphioxeia* per *M. rubrum* d^{-1} (Smith and Hansen, 2007). *Dinophysis* and *M. rubrum* were both fed at a predator: prey ratio of 1:10 in this study which, coupled with carbon uptake through photosynthesis and growth in nutrient-replete media, should have provided ample nutrients and prey to sustain maximum growth rates for the duration of experiments (1–3 weeks). Growth of *T. amphioxeia*, having been maintained in nutrient-replete L1 media, should not have been limited by nutrient availability, either.

The growth response of *M. rubrum* to temperature and salinity was generally similar to that of the two strains of *T. amphioxeia*. This is not surprising, given *M. rubrum* sequesters prey chloroplasts and nuclei and is primarily photoautotrophic (Smith and Hansen, 2007). In most treatments *M. rubrum* was able to clear or control prey abundance by the end of the experiment. When grown at 27 °C, *M. rubrum* failed to eliminate or control *T. amphioxeia* growth. At 27 °C and 50 µmol quanta $m^{-2} s^{-1}$ growth rates could not be obtained for *M. rubrum* because of mortality. *Mesodinium rubrum* is sensitive to pH above 8.8 (Hansen and Fenchel, 2006; Park et al., 2006). Though the pH of culture media was not measured during these experiments, it is possible *T. amphioxeia* outgrew the grazing pressure of *M. rubrum* at these conditions, altering the pH of the media and leading to mortality of *M. rubrum*. Although pH may have been the ultimate cause of *M. rubrum* mortality, suppressed growth and grazing rates of *M. rubrum* due to the conditions at which they were grown allowed *T. amphioxeia* to proliferate and change the pH of the media. At 27 °C and irradiance treatments above 50 µmol quanta $m^{-2} s^{-1}$, *M. rubrum* survived for the duration of the experiment. At 27 °C, *M. rubrum* clearly begins to struggle, while *T. amphioxeia* appears to be capable of growing well at this temperature.

The physiological relationship between *M. rubrum* and its sequestered organelles may be the cause of this sensitivity to warm temperature. In addition to kleptochloroplasts, *M. rubrum* cells contain a single large central prey nucleus and several smaller nuclei which *M. rubrum* uses to control sequestered chloroplasts (Johnson et al., 2007). The smaller nuclei are distributed around the periphery of the cell, and are passed to new cells during cell division, where they enlarge and become central nuclei in daughter cells (Kim et al., 2017). These nuclei are transcriptionally active, and many genes relating to chlorophyll synthesis, light and dark reactions, and DNA methylation are up-regulated relative to *T. amphioxeia* (Kim et al., 2016). This alteration of gene expression and function, coupled with the fact that a few nuclei may be supporting as many as 20 kleptochloroplasts (Kim et al., 2017), may explain the sensitivity to high temperature observed in *M. rubrum*. As temperatures rise, *M. rubrum* may be unable to maintain kleptochloroplasts. Whether different prey items may be more tolerant to higher temperatures is unknown.

The two geographically distinct species of *Dinophysis* used in these experiments, *D. acuminata* (DAVA01) from Chesapeake Bay and *D. ovum* (DoSS3195) from Surfside Beach, TX, are generally similar with regard to growth rates across the range of salinities, temperatures, and irradiances tested. DAVA01 does, however, grow at a consistently higher rate than DoSS3195 at 100 µmol quanta $m^{-2} s^{-1}$ and 12 °C. At this temperature growth of DoSS3195 decreases relative to growth rates at 18 °C while growth of DAVA01 is more stable. The results of t-tests with

Benjamini-Hochberg corrected p-values show most significantly different growth rates between these species occurred at 12 °C (Supplementary Table 2). These differences may be explained by adaptation of geographically distinct species to conditions characteristic of their region. DAVA01, being a temperate species, is likely more capable of maintaining growth at low temperatures in comparison with the subtropical DoSS3195.

Suitability of prey may also influence the growth response of *Dinophysis*. Both *Dinophysis* strains were fed the Danish *T. amphioxeia* and a Danish strain of *M. rubrum* to isolate the growth response to environmental factors alone. It may be the case that these foreign prey organisms were functional but not ideal for either the subtropical *D. ovum* or the temperate *D. acuminata*. *Dinophysis* and *Mesodinium* are capable of limited control over their kleptochloroplasts (Moeller et al., 2011; Hansen et al., 2016; Rusterholz et al., 2017). The ability of *Dinophysis* and *Mesodinium* to photosynthesize and control their kleptochloroplasts may depend upon their source. *Mesodinium rubrum* can swap chloroplasts depending on available prey, and growth rates are not constant for all species of cryptophyte (Park et al., 2007; Myung et al., 2011). Variable growth responses have been observed in *Mesodinium* and *Dinophysis* when fed geographically distinct cryptophyte isolates (Hernández-Urcera et al., 2018). The differential growth response of the *Dinophysis* species used in these experiments may be due to their individual affinity for the specific cryptophyte prey provided. Additional experiments regarding the prey selectivity and suitability of *Dinophysis, Mesodinium*, and *Teleaulax* species are needed to address this question.

The exact mechanism of control of acquired chloroplasts by *Dinophysis* may cause differences in the growth response to temperature and irradiance. In *M. rubrum*, the chloroplasts of cryptophytes are sequestered along with other organelles, including the cryptophyte nucleus which helps control and maintain kleptochloroplasts. Unlike *M. rubrum, Dinophysis* digests all of the material from its prey and retains only the chloroplasts (Park et al., 2008; Kim et al., 2012). *Dinophysis* is capable of some control over its captured chloroplasts, including division of kleptochloroplasts, without retaining nuclei from prey (Rusterholz et al., 2017). They may therefore be less able to regulate their kleptochloroplasts, resulting in sensitivity to high or low temperature and damaging irradiance. Degradation of kleptochloroplasts in *Dinophysis* cells is correlated with light intensity (Rusterholz et al., 2017). In these experiments both *Dinophysis* species achieved maximum growth at around 100 µmol quanta $m^{-2} s^{-1}$ in most treatments. This plateau may have been due to degradation of kleptochloroplasts at irradiances above 100 µmol quanta $m^{-2} s^{-1}$. The ability of *Dinophysis* to heavily supplement its carbon and nutrient intake with heterotrophy may balance their inability to maintain kleptochloroplasts as well as *M. rubrum*.

Both DAVA01 and DoSS3195 exhibited spikes in growth rates at the two higher salinities tested (30 for DoSS3195 and 34 for DAVA01) when grown at 24 °C. Growth rates of *M. rubrum* and both strains of *T. amphioxeia* were highest at this temperature or beginning to plateau. In these experiments *Dinophysis* were fed prey which had been acclimated to the experimental treatment conditions at which *Dinophysis* were being tested. At these conditions, *Dinophysis* may capture optimal chloroplasts which are either photosynthesizing most efficiently or providing *Dinophysis* with an abundance of an essential growth factor. It has been shown that *Dinophysis* growth is related to the physiological state of *M. rubrum* (Riisgaard and Hansen, 2009). If, at these conditions, *Dinophysis* are consuming ideal prey their growth rates may be enhanced. Otherwise, the trend in growth rate of both species of *Dinophysis* is generally negative with increasing salinity.

4.2. Ecological implications for bloom initiation in the Gulf of Mexico

The strong response and tolerance of *T. amphioxeia* growth to warm temperatures suggest abundances may be seasonal, but they should be capable of surviving throughout the year. Given the low threshold of ingestion required for *M. rubrum* to maintain maximum growth and the ability of *T. amphioxeia* to grow reliably across the range of conditions tested, *M. rubrum* should have prey available throughout the year especially if they can consume a variety of other cryptophytes. In fact, both these taxa have been observed year-round in the Gulf of Mexico by the Texas Observatory for Algal Succession Time Series (toast.tamu.edu/IFCB7).

The ciliate *M. rubrum* is known to form seasonal blooms around the world. In the Gulf of Mexico, these blooms usually occur between September and February (Harred and Campbell, 2014). In Chesapeake Bay, *M. rubrum* blooms occur in the Spring and Fall, as well, and are often associated with specific temperature and salinity ranges (Johnson et al., 2013). In these experiments *M. rubrum* grew fastest at 18 – 24 °C and salinity 30 – 34, with differences in growth primarily driven by temperature and irradiance. The ranges observed for maximal growth of *M. rubrum* in these experiments overlap well with the range of temperature and salinity observed for *M. rubrum* bloom onset in the Gulf of Mexico (23 – 29 °C, salinity 30 – 34, Harred and Campbell, 2014). The significant decreases in growth rates observed above 24 °C suggests a strong sensitivity of *M. rubrum* growth to warm temperatures. This sensitivity to warm temperatures can explain the timing of blooms of *M. rubrum* and their relative absence in summer months when coastal waters in the Gulf of Mexico approach 30 °C (Fig. 1). During the period between September and January, water temperatures in the Gulf of Mexico (Fig. 1) fall into the range within which blooms of *M. rubrum* have been observed (Harred and Campbell, 2014).

The timing of blooms of both predator and prey may be linked. *Mesodinium* species and *Teleaulax* are known to co-occur prior to blooms of *Mesodinium* (Peterson et al., 2013; Herfort et al., 2017), and *Dinophysis* blooms are often preceded by high abundances of *Mesodinium*, including in the Gulf of Mexico (Campbell et al., 2010; Diaz et al., 2013; Harred and Campbell, 2014; Velo-Suárez et al., 2014; Moita et al., 2016). In these experiments, maximal growth of both strains of *Teleaulax* fell within the range reported for *M. rubrum* blooms in the Gulf of Mexico (23 – 29 °C, salinity 30 – 34, Harred and Campbell, 2014). Blooms of *M. rubrum* in the Gulf of Mexico may be the result of ideal growth conditions between September and January and an abundance of rapidly growing prey. Both *Dinophysis* and *Mesodinium* grow well between 18 and 24 °C, suggesting an overlap of predator and prey is possible, as well.

The relationship between *Dinophysis* and its prey is complicated. Currently, successful cultures have only been established using *M. rubrum* and cryptophytes belonging to the *Teleaulax / Plagioselmis / Geminigera* clade. It is still unknown to what extent *Dinophysis* may utilize different types of plastids or prey upon different ciliates. There are several species of *M. rubrum* which may or may not be suitable prey for *Dinophysis* (Garcia-Cuetos et al., 2012). Evidence of plastids other than *Teleaulax*, including haptophyte, raphidophyte, and chlorophyte plastids, have also been found in *Dinophysis* cells (Qiu et al., 2011; Kim et al., 2012; Stern et al., 2014). *Dinophysis* may be capable of consuming other organisms, with implications for growth and bloom formation if different prey are more or less favorable for *Dinophysis* growth. The strongest relationship between *Dinophysis* blooms and prey still appears to be with the ciliate *M. rubrum* and its cryptophyte prey.

The results of these experiments show that DoSS3195 growth is most sensitive to temperature variability and grows best at low salinity (22) and moderate temperature (18 – 24 °C). In comparison, temperature, salinity, and irradiance all affect DAVA01 growth to a similar degree (Supplementary Table 1). Harred and Campbell (2014) reported the temperature and salinity range within which *Dinophysis* blooms occurred to be 11 – 19 °C and salinity 28 – 33. The actual temperature range may be slightly higher, at 18 – 24 °C. In fact, growth of the *D. ovum* isolate was suppressed at temperatures below 18 °C. Above 24 °C, both species struggled to survive.

Sensitivity to warm waters may explain why *D. ovum* blooms do not typically occur in the fall despite the propensity for blooms of *M. rubrum* to occur during the period of cooling surface waters between September and January in the Gulf of Mexico (Fig. 1). High summer temperatures in the Gulf of Mexico may cause mortality of any *D. ovum* cells in surface waters, and populations may retreat to deeper, cooler waters on the outer Texas-Louisiana shelf, residing near fronts (Pitcher et al., 1998), the pycnocline (Moita et al., 2006; Velo-Suárez et al., 2008), or retentive structures like eddies (Xie et al., 2007). Currents along the Texas coast during summer are generally northeastward, promoting upwelling and offshore Ekman transport, as well (Cochrane and Kelly, 1986). Though temperatures may fall within the optimal range for *D. ovum* growth during the transition from summer to winter, and a return to downcoast currents promotes onshore transport (Cochrane and Kelly, 1986), weakening of stratification and mixing as surface waters cool may disperse *D. ovum* cells and prevent population growth. However, these offshore holoplanktonic populations of *D. ovum* may still serve as an inoculum for the observed seasonal spring blooms along the Texas coast (Smayda and Trainer, 2010). The source of *D. ovum* inoculum populations in the Gulf of Mexico is currently unknown and should be investigated further to improve bloom forecasting.

The salinity range during *Dinophysis* blooms in the Gulf of Mexico was reported to be between 28 and 33 (Harred and Campbell, 2014). The actual range of optimal salinities, according to the results of the growth experiments described herein, is likely lower, between 22 and 26 salinity. Salinity may be far less important in the development of blooms than temperature based on ANOVA results, although the temperate DAVA01 showed greater sensitivity to differences in salinity than DoSS3195. Mean salinity at 5 – 7 m in the Mission Aransas Shipping Channel falls within a stable range (~30 – 34, Fig. 1) throughout the year, though variance of salinity data suggests salinities below 30 are not uncommon. The narrow salinity range observed at the Mission Aransas Shipping Channel suggests temperature is the primary factor controlling *Dinophysis* blooms in the Gulf of Mexico.

The results of these growth experiments suggest a potential series of seasonal events that could lead to blooms of *D. ovum* in the Gulf of Mexico. In the summer, warm temperatures cause mortality of *D. ovum* in surface waters. Upwelling and offshore Ekman transport, combined with mortality due to warm surface waters, may restrict populations of *D. ovum* to offshore fronts and retentive structures. *Teleaulax amphioxeia* and *M. rubrum* can survive the summer in surface waters, however. During the fall and winter, as surface waters cool, *M. rubrum* consumes *T. amphioxeia* and blooms. *Dinophysis ovum* may graze on healthy *M. rubrum* populations, gathering kleptochloroplasts and dividing, but mixing and breakdown of water column stratification dilutes cells faster than the rate of population increase, especially if temperatures drop below 18 °C which may suppress *D. ovum* growth rates. In spring (January – May), as surface waters warm and stratify, *D. ovum* populations may again gather at the pycnocline. Crucially, as temperatures enter the ideal range for growth and if *D. ovum* encounter sufficient prey and optimal salinity conditions populations may grow rapidly, increasing the probability of a bloom occurring. Downwelling-favorable currents (Cochrane and Kelly, 1986) and tidal activity may transport these populations into coastal bays. The culturing experiments herein demonstrate that while physical processes may deliver populations of *D. ovum* to the Texas coast, the intensity of *D. ovum* blooms may be highly dependent upon favorable growth conditions.

4.3. Phylogenies and toxin profiles

The two *Dinophysis* species in this study were distinct in their toxin profiles. Differences were clear regarding the intracellular toxin composition, with *D. acuminata* containing OA, DTX1, and PTX2 and *D. ovum* only containing OA. This finding agreed with previous studies involving field populations of *Dinophysis* (Deeds et al., 2010; Wolny et al., 2020) and other laboratory strains of these two species (Fux et al., 2011; Smith et al., 2018). Additionally, *D. ovum* may pose more of a threat to seafood safety because a single cell contained almost two orders of magnitude more DSP toxin than *D. acuminata* when grown under the same conditions.

Toxin variability among *Dinophysis* species is extensive (Reguera et al., 2014 and references therein). The DAVA01 isolate of *D. acuminata* used in this study has a toxin profile like other isolates of the same species from the northeastern United States and similar to the toxin profile of *D. sacculus* isolated from Spanish waters (Riobó et al., 2013). The DoSS3195 isolate of *D. ovum* has a toxin profile unique among North American populations of *Dinophysis*. DoSS3195 produced only OA at detectable levels, while toxin profiles of *Dinophysis* from the mid-Atlantic region of the United States are characterized by PTX2, OA and DTX1 (Wolny et al., 2020) and west coast *Dinophysis* species may produce OA, DTX1, DTX2, and PTX2 based on studies of toxin concentrations in shellfish tissue (Trainer et al., 2013; Shultz et al., 2019). The toxin profile of DoSS3195 was consistent with toxin analyses performed during the 2008 bloom of *D. ovum* in Texas, in which only OA was found in oyster tissue and seawater (Deeds et al., 2010). Additional experiments investigating the production and role of toxins by regional isolates of *Dinophysis* are necessary to reveal drivers of toxin variability.

Although these *Dinophysis* species are physiologically remarkably distinct based on their toxin profiles, they were not distinguishable genetically using the ITS, LSU, *cox1*, and *cob* genes tested here or in recent studies (Raho et al., 2013; Park et al., 2020; Wolny et al., 2020). The *cob* and *cox1* genes used in this study resulted in a similar grouping of several *Dinophysis* species within the *D. acuminata* complex. While *cob* has been determined to be useful for inferring dinoflagellate phylogeny (Zhang et al., 2005), its utility is limited for *Dinophysis* species due to the few sequences currently available. The phylogenetic relationship of species within the *D. acuminata* complex is consistent for DAVA01 and DoSS3195. Recent morphological studies came to conflicting conclusions regarding whether *D. acuminata* and *D. ovum* can be distinguished by physical characteristics (Park et al., 2020; Wolny et al., 2020). Conflicting conclusions over the taxonomy *of D. acuminata and D. ovum* emphasizes the need for a reliable molecular marker to identify *Dinophysis* species.

5. Conclusions

In this study the results of extensive experiments designed to test the growth response of two geographically distinct isolates of *Dinophysis*, one isolate of *Mesodinium*, and two isolates of *T. amphioxeia* to a range of temperature, salinity, and irradiance treatments were presented. Optimal conditions for growth of *Teleaulax* and *Mesodinium* were found to be 24 °C, 300 – 400 μmol quanta $m^{-2} s^{-1}$, and salinities above 30. *Dinophysis* isolates grew best at moderate temperatures (18 – 24 °C) and lower salinities (22 – 26), with distinct spikes in growth rate at 24 °C associated with specific salinities. The two *Dinophysis* isolates responded differently to the factors tested; temperature most impacted *D. ovum* growth while the effects of temperature, irradiance, and salinity on the growth of *D. acuminata* were comparable. Temperatures above 24 °C suppressed growth rates or were fatal for *Mesodinium* and *Dinophysis*. In the Gulf of Mexico, *D. ovum* growth is likely enhanced by warming temperatures during the shift in seasons from winter to spring and further elevated if salinity falls within a narrow range, with implications for bloom intensity. In addition to differences in growth, the toxin profiles of *D. acuminata* and *D. ovum* are markedly different. While *D. acuminata* and *D. ovum* may be distinguished physiologically, commonly used genes are insufficient to differentiate species within the *D. acuminata* species complex.

Declaration of Competing Interest

The authors declare that they have no known competing financial interests or personal relationships that could have appeared to

influence the work reported in this paper.

Acknowledgements

Teleaulax (K-0434, Scandinavian Cultures Collection of Algae and Protozoa) and *M. rubrum* (MBL-DK2009) cultures were isolated from Helsingør Harbor, Denmark, and were generously provided by Dr. P.J. Hansen. Authors express gratitude to Dr. Darren W. Henrichs for help with culturing and isolating the GoMTA strain of *T. amphioxeia*. Many thanks to Dr. Claude Mallet (Waters, Inc.) for his valuable advice and generous donation of the Xevo MS. Authors would also like to express gratitude to Marta Sanderson, Dr. Nour Ayache, and Dr. Han Gao (VIMS) for their assistance in culture maintenance and toxin analysis. Thank you to Dr. Chetan Gaonkar for help with phylogenetic analysis, preparation of DNA sequences, and editing this paper. Finally, the authors express thanks to Linnea Hetland and Teresa Kenny for their help with cell counts during growth experiments.

Funding

Publication supported in part by an Institutional Grant NA14OAR4170102 to the Texas Sea Grant College Program from the National Sea Grant Office, National Oceanic and Atmospheric Administration, U.S. Department of Commerce awarded to L.C. (TAMU). Partial support for this research was also received from the National Oceanic and Atmospheric Administration National Centers for Coastal Ocean Science Competitive Research Program under award NA17NOS4780184 to L.C. (TAMU) and J.L.S. (VIMS). This paper is ECOHAB contribution number ECO966.

Supplementary materials

Supplementary material associated with this article can be found, in the online version, at doi:10.1016/j.hal.2020.101896.

References

Aubry, F.B., Berton, A., Bastianini, M., Bertaggia, R., Baroni, A., Socal, G., 2000. Seasonal dynamics of *Dinophysis* in coastal waters of the NW Adriatic Sea (1990-1996). Bot. Mar. 43 (5), 423–430.

Benjamini, Y., Hochberg, Y., 1995. Controlling the false discovery rate: a practical and powerful approach to multiple testing. J. R. Stat. Soc. B 57 (1), 289–300.

Campbell, L., Olson, R.J., Sosik, H.M., Abraham, A., Henrichs, D.W., Hyatt, C.J., Buskey, E.J., 2010. First harmful *Dinophysis* (DINOPHYCEAE, DINOPHYSIALES) bloom in the US is reavealed by automated imaging flow cytometry. J. Phycol. 46 (1), 66–75.

Cochrane, J.D., Kelly, F.J., 1986. Low-frequency circulation on the Texas-Louisiana continental shelf. J. Geophys. Res. 91 (C9) 10,645-10,659.

Core Team, R., 2019. R: A language environment for statistical computing. R Foundation for Statistical Computing, Vienna, Austria URL. http://www.R-project.org/.

Dahl, E., Aune, T., Aase, B., 1996. Reddish water due to mass occurrence of *Dinophysis* spp. Intergovernmental Oceanographic Commision of UNESCO, Paris, France, pp. 265–267.

Deeds, J.R., Wiles, K., Heideman VI, G.B., White, K.D., Abraham, A., 2010. First US report of shellfish harvesting closures due to confirmed okadaic acid in Texas Gulf coast oysters. Toxicon 55 (6), 1138–1146.

Diaz, P.A., Reguera, B., Ruiz-Villarreal, M., Pazos, Y., Velo-Suárez, L., Berger, H., Sourisseau, M., 2013. Climate variability and oceanographic settings associated with interannual variability in the initiation of *Dinophysis acuminata* blooms. Mar. Drugs 11 (8), 2964–2981.

Edler, D., Klein, J., Antonelli, A., Silvestro, D., 2019. raxmlGUI 2.0 beta: a graphical interface and toolkit for phylogenetic analyses using RAxML. bioRxiv, 800912.

Fujiki, H., Suganuma, M., Suguri, H., Yoshizawa, S., Takagi, K., Uda, N., Wakamatsu, K., Yamada, K., Murata, M., Yasumoto, T., Sugimura, T., 1988. Diarrhetic shellfish toxin, dinophysistoxin-1, is a potent tumor promoter on mouse skin. Jpn. J. Cancer Res. 79 (10), 1089–1093.

Fux, E., Smith, J.L., Tong, M., Guzmán, L., Anderson, D.M., 2011. Toxin profiles of five geographical siolates of *Dinophysis* spp. from North and South America. Toxicon 57 (2), 275–287.

Garcia-Cuetos, L., Moestrup, Ø., Hansen, P.J., 2012. Studies on the genus *Mesodinium* II. ultrastructural and molecular investigations of five marine species help clarifying the taxonomy. J. Eukaryot. Microbiol 59 (4), 374–400.

Gouy, M., Guindon, S., Gascuel, O., 2010. SeaView version 4: a multiplatform graphical user interface for sequence alignment and phylogenetic tree building. Mol. Biol. Evol. 27 (2), 221–224.

Guillard, R.R.L., 1973. Division Rates. In: Stein, J.R. (Ed.), Handbook of phycological methods. Cambridge University Press, Cambridge, pp. 289–312.

Guillard, R.R.L., Hargraves, P.E., 1993. *Stichochrysis immobilis* is a diatom, not a chrysophyte. Phycologia 32 (3), 234–236.

Hall, T.A., 1999. BioEdit: a user-friendly biological sequence alignment editor and analysis program for Windows 95/98/NT. Nucl. Acids. Symp. Ser. 41, 95–98.

Hallegraeff, G.M., Lucas, I.A.N., 1988. The marine dinoflagellate genus *Dinophysis* (Dinophyceae): photosynthetic, neritic and non-photosynthetic, oceanic species. Phycologia 27 (1), 25–42.

Hansen, P.J., Fenchel, T., 2006. The bloom-forming ciliate *Mesodinium rubrum* harbours a single permanent endosymbiont. Mar. Biol. Res 2 (3), 169–177.

Hansen, P.J., Moldrup, M., Tarangkoon, W., Garcia-Cuetos, L., Moestrup, Ø, 2012. Direct evidence for symbiont sequestration in the marine red tide ciliate *Mesodinium rubrum*. Aquat. Microb. Ecol 66 (1), 63–75.

Hansen, P.J., Ojamäe, K., Berge, T., Trampe, E.C.L., Nielsen, L.T., Lips, I., Kühl, M., 2016. Photoregulation in a kleptochloroplastidic dinoflagellate, *Dinophysis acuta*. Front. Microbiol 7, 785.

Harred, L.B., Campbell, L., 2014. Predicting harmful algal blooms: a case study with *Dinophysis ovum* in the Gulf of Mexico. J. Plankton Res 36 (6), 1434–1445.

Hattenrath-Lehmann, T.K., Marcoval, M.A., Berry, D.L., Fire, S., Wang, Z., Morton, S.L., Gobler, C.J., 2013. The emergence of *Dinophysis acuminata* blooms and DSP toxins in shellfish in New York waters. Harmful Algae 26, 33–44.

Herfort, L., Maxey, K., Voorhees, I., Simon, H.M., Grobler, K., Peterson, T.D., Zuber, P., 2017. Use of highly specific molecular markers reveals positive correlation between abundances of *Mesodinium* cf. *major* and its preferred prey, *Teleaulax amphioxeia*, during red water blooms in the Columbia River estuary. J. Eukaryot. Microbiol. 64 (6), 740–755.

Hernández-Urcera, J., Rial, P., Garcia-Portela, M., Lourés, P., Kilcoyne, J., Rodriguez, F., Fernández-Villamarin, A., Reguera, B., 2018. Notes on the cultivation of two mixotrophic *Dinophysis* species and their ciliate prey *Mesodinium rubrum*. Toxins (Basel) 10 (12), 505.

Hetland, R.D., Campbell, L., 2007. Convergent blooms of *Karenia brevis* along the Texas coast. Geophys. Res. Lett 34 (19), L19604.

Jester, R., Lefebvre, K., Langlois, G., Vigilant, V., Baugh, K., Silver, M.W., 2009. A shift in the dominant toxin-producing algal species in central California alters phycotoxins in food webs. Harmful Algae 8 (2), 291–298.

Johnson, M.D., Oldach, D., Delwiche, C.F., Stoecker, D.K., 2007. Retention of transcriptionally active cryptophyte nuclei by the ciliate *Myrionecta rubra*. Nature 445, 426–428.

Johnson, M.D., Stoecker, D.K., Marshall, H.G., 2013. Seasonal dynamics of *Mesodinium rubrum* in Chesapeake Bay. J. Plankton Res 35 (4), 877–893.

Kat, M., 1983. Diarrhetic mussel poisoning in the Netherlands related to the dinoflagellate *Dinophysis acuminata*. Antonie Van Leeuwenhoek 49 (4–5), 417–427.

Kim, S., Kang, Y.G., Kim, H.S., Yih, W., Coats, D.W., Park, M.G., 2008. Growth and grazing responses of the mixotrophic dinoflagellate *Dinophysis acuminata* as functions of light intensity and prey concentration. Aquat. Microb. Ecol 51 (3), 301–310.

Kim, M., Kim, S., Yih, W., Park, M.G., 2012. The marine dinoflagellate genus *Dinophysis* can retain plastids of multiple algal origins at the same time. Harmful Algae 13, 105–111.

Kim, G.H., Han, J.H., Kim, B., Han, J.W., Nam, S.W., Shin, W., Park, J.W., Yih, W., 2016. Cryptophyte gene regulation in the kleptoplastidic, karyokleptic ciliate *Mesodinium rubrum*. Harmful Algae 52, 23–33.

Kim, M., Drumm, K., Daugbjerg, N., Hansen, P.J., 2017. Dynamics of sequestered cryptophyte nuclei in *Mesodinium rubrum* during starvation and refeeding. Front. Microbiol 8, 423.

Kim, M., Nam, S.W., Shin, W., Coats, D.W., Park, M.G., 2012. *Dinophysis caudata* (Dinophyceae) sequesters and retains plastids from the mixotrophic ciliate prey *Mesodinium rubrum*. J. Phycol. 48 (3), 569–579.

Koike, K., Nishiyama, A., Takishita, K., Kobiyama, A., Ogata, T., 2007. Appearance of *Dinophysis fortii* following blooms of certain cryptophyte species. Mar. Ecol. Prog. Ser 337, 303–309.

Kumar, S., Stecher, G., Li, M., Knyaz, C., Tamura, K., 2018. MEGA X: molecular evolutionary genetics analysis across computing platforms. Mol. Biol. Evol 35, 1547–1549.

Levene, H., 1960. Robust tests for equality of variances. In: Olkin, I. (Ed.), Contributions to probability and statistics. Stanford University Press, Redwood City, CA, pp. 278–292.

Lin, S., Zhang, H., Spencer, D.F., Norman, J.E., Gray, M.W., 2002. Widespread and extensive editing of mitochondrial mRNAS in dinoflagellates. J. Mol. Biol. 320 (4), 727–739.

Lüdecke, D. (2020). sjstats: statistical functions for regression models (Version 0.17.9).

Maranda, L., Shimizu, Y., 1987. Diarrhetic shellfish poisoning in Narragansett Bay. Estuaries 10, 298–302.

Maxwell, D.P., Falk, S., Trick, C.G., Huner, N.P.A., 1994. Growth at low temperature mimics high-light acclimation in *Chlorella vulgaris*. Plant Physiol 105 (2), 535–543.

McKinney, W., 2010. Data structures for statistical computing in Python. In: Proceedings of the 9th Python in Science Conference, pp. 51–56.

Medlin, L., Elwood, H.J., Stickel, S., Sogin, M.L., 1988. The characterization of enzymatically amplified eukaryotic 16S-like rRNA-coding regions. Gene 71 (2), 491–499.

Moeller, H.V., Johnson, M.D., Falkowski, P.G., 2011. Photoacclimation in the phototrophic marine ciliate *Mesodinium rubrum* (CILIOPHORA). J. Phycol 47 (2), 324–332.

Moita, M.T., Sobrinho-Conçalves, Oliveria, P.B., Palma, S., Falcão, M., 2006. A bloom of *Dinophysis acuta* in a thin layer off North-West Portugal. Afr. J. Mar. Sci 28, 265–269.

Moita, M.T., Pazos, Y., Rocha, C., Nolasco, R., Oliveira, P.B., 2016. Toward predicting *Dinophysis* blooms off NW Iberia: a decade of events. Harmful Algae 53, 17–32.

Myung, G., Kim, H.S., Park, J.S., Park, M.G., Yih, W., 2011. Population growth and plastid

type of *Myrionecta rubra* depend on the kinds of available cryptomonad prey. Harmful Algae 10 (5), 536–541.
Myung, G., Kim, H.S., Park, J.W., Park, J.S., Wonho, Y., 2013. Sequestered plastids in *Mesodinium rubrum* are functionally active up to 80 days of phototrophic growth without cryptomonad prey. Harmful Algae 27, 82–87.
NOAA National Estuarine Research Reserve System (NERRS). System-wide monitoring program. Data accessed from the NOAA NERRS Centralized Data Management Office website:Www.nerrsdata.orgAccessed [7 June 2019].
Olejnik, S., Algina, J., 2003. Generalized eta and omega squared statistics: measures of effect size for some common research designs. Psychol. Methods 8 (4), 434–447.
Onofrio, M.D., Mallet, C.R., Place, A.R., Smith, J.L., 2020. A screening tool for the direct analysis of marine and freshwater phycotoxins in organic SPATT extracts from the Chesapeake Bay. Toxins (Basel) 12 (5), 322.
Pan, Y., Cambella, A.D., Quilliam, M.A., 1999. Cell cycle and toxin production in the benthic dinoflagellate *Prorocentrum lima*. Mar. Biol 134, 541–549.
Park, M.G., Kim, S., Kim, H.S., Myung, G., Kang, Y.G., Yih, W., 2006. First successful culture of the marine dinoflagellate *Dinophysis acuminata*. Aquat. Microb. Ecol 45 (2), 101–106.
Park, J.S., Myung, G., Kim, H.S., Cho, B.C., Yih, W., 2007. Growth responses of the marine photosynthetic ciliate *Myrionecta rubra* to different cryptomonad strains. Aquat. Microb. Ecol 48 (1), 83–90.
Park, M.G., Park, J.S., Kim, M., Yih, W., 2008. Plastid dynamics during survival of *Dinophysis caudata* without its ciliate prey. J. Phycol 44 (5), 1154–1163.
Park, J.H., Kim, M., Jeong, H.J., Park, M.G., 2020. Revisiting the taxonomy of the "*Dinophysis acuminata* complex" (Dinophyta). Harmful Algae 88, 101657.
Peterson, T.D., Golda, R.L., Garcia, M.L., Li, B., Maier, M.A., Needoba, J.A., Zuber, P., 2013. Associations between *Mesodinium rubrum* and cryptophyte algae in the Columbia River estuary. Aquat. Microb. Ecol 68 (2), 117–130.
Pitcher, G.C., Boyd, A.J., Horstman, D.A., Mitchell-Innes, B.A., 1998. Subsurface dinoflagellate populations, frontal blooms and the formation of red tide in the southern Benguela upwelling system. Mar. Ecol. Prog. Ser. 172, 253–264.
Qiu, D., Huang, L., Liu, S., Lin, S., 2011. Nuclear, mitochondrial and plastid gene phylogenies of *Dinophysis miles* (Dinophyceae): evidence of variable types of chloroplasts. PLoS ONE 6 (12).
Raho, N., Rodríguez, F., Reguera, B., Marín, I., 2013. Are the mitochondrial *cox1* and *cob* genes suitable markers for species of *Dinophysis* Ehrenberg? Harmful Algae 28, 64–70.
Reguera, B., Velo-Suárez, L., Raine, R., Park, M.G., 2012. Harmful *Dinophysis* species: a review. Harmful Algae 14, 87–106.
Reguera, B., Riobó, P., Rodriguez, F., Diaz, P.A., Pizarro, G., Paz, B., Franco, J.M., Blanco, J., 2014. *Dinophysis* toxins: causative organisms, distribution and fate in shellfish. Mar. Drugs 12 (1), 394–461.
Riisgaard, K., Hansen, P.J., 2009. Role of food uptake for photosynthesis, growth and survival of the mixotrophic dinoflagellate *Dinophysis acuminata*. Mar. Ecol. Prog. Ser 381, 51–62.
Riobó, P., Reguera, B., Franco, J.M., Rodríguez, F., 2013. First report of the toxin profile of *Dinophysis sacculus* Stein from LC-MS analysis of laboratory cultures. Toxicon 76, 221–224.
Rogers, S.O., Bendich, A.J., 1994. Extraction of total cellular DNA from plants, algae and fungi. In: Gelvin, S.B., Schilperoort, R.A. (Eds.), Plant Molecular Biology Mannual Second Edition. Springer Science + Business Media, B.V., Dordrecht, pp. 183–190.
Rusterholz, P.M., Hansen, P.J., Daugbjerg, N., 2017. Evolutionary transition towards permanent chloroplasts? – division of kleptochloroplasts in starved cells of two species of *Dinophysis* (Dinophyceae). PLoS ONE 12 (5), e0177512.
Scholin, C.A., Herzog, M., Sogin, M., Anderson, D.M., 1994. Identification of group- and strain-specific genetic markers for globally distributed *Alexandrium* (Dinophyceae). II. sequence analysis of a fragment of the LSU rRNA gene. J. Phycol 30, 999–1011.
Shultz, D., Campbell, L., Kudela, R.M., 2019. Trends in *Dinophysis* abundance and diarrhetic shellfish toxin levels in California mussels (*Mytilus californianus*) from Monterey Bay, California. Harmful Algae 88, 101641.
Sievers, F., Wilm, A., Dineen, D., Gibson, T.J., Karplus, K., Li, W., Lopez, R., McWilliam, H., Remmert, M., Söding, J., Thompson, J.D., Higgins, D.G., 2011. Fast, scalable generation of high-quality protein multiple sequence alignments using Clustal Omega. Mol. Syst. Biol. 7, 539.
Silvestro, D., Michalak, I., 2012. raxmlGUI: a graphical front-end for RAxML. Org. Divers. Evol. 12, 335–337.
Smayda, T.J., Trainer, V.L., 2010. Dinoflagellate blooms in upwelling systems: seeding, variability, and contrasts with diatom bloom behavior. Prog. Oceanogr. 85 (1–2), 92–107.
Smith, M., Hansen, P.J., 2007. Interaction between *Mesodinium rubrum* and its prey: importance of prey concentration, irradiance and pH. Mar. Ecol. Prog. Ser 338, 61–70.
Smith, J.L., Tong, M., Kulis, D., Anderson, D.M., 2018. Effect of ciliate strain, size, and nutritional content on the growth and toxicity of mixotrophic *Dinophysis acuminata*. Harmful Algae 78, 95–105.
Stamatakis, A., 2014. RAxML version 8: a tool for phylogenetic analysis and post-analysis of large phylogenies. Bioinformatics 30 (9), 1312–1313.
Stern, R.F., Amorim, A.L., Bresnan, E., 2014. Diversity and plastid types in *Dinophysis acuminata* complex (Dinophyceae) in Scottish waters. Harmful Algae 39, 223–231.
Stoecker, D.K., Hansen, P.J., Caron, D.A., Mitra, A., 2017. Mixotrophy in the marine plankton. Annu. Rev. Mar. Sci. 9, 311–335.
Tamura, K., Stecher, G., Peterson, D., Filipski, A., Kumar, S., 2013. MEGA6: molecular evolutionary genetics analysis version 6.0. Mol. Biol. Evol 30 (12), 2725–2729.
Ten-Hage, L., Delaunay, N., Pichon, V., Couté, A., Puiseux-Dao, S., Turquet, J., 2000. Okadaic acid production from the marine benthic dinoflagellate *Prorocentrum arenarium* Faust (Dinophyceae) isolated from Europa Island coral reef ecosystem (SW Indian Ocean). Toxicon 38 (8), 1043–1054.
Trainer, V.L., Moore, L., Bill, B.D., Adams, N.G., Harrington, N., Borchert, J., Da Silva, D.A.M., Eberhart, B-T.L., 2013. Diarrhetic shellfish toxins and other lipophilic toxins of human health concern in Washington State. Mar. Drugs 11 (6), 1815–1835.
van Rossum, G., Drake, F.L. (Eds.), 2011. The Python language reference manual. Network Theory Limited.
Velo-Suárez, L., González-Gil, S., Gentien, P., Lunven, M., Bechemin, C., Fernand, L., Raine, R., Reguera, B., 2008. Thin layers of *Pseudo-nitzschia* spp. and the fate of *Dinophysis acuminata* during an upwelling-downwelling cycle in a Galician Ría. Limnol. Oceanogr 53, 1815–1834.
Velo-Suárez, L., González-Gil, S., Reguera, B., 2014. The growth season of *Dinophysis acuminata* in an upwelling system embayment: a conceptual model based on in situ measurements. Deep-Sea Res. Pt. II. 101, 141–151.
Virtanen, P., Gommers, R., Oliphant, T.E., Haberland, M., Reddy, T., Cournapeau, D., Burovski, E., Peterson, P., Weckesser, W., Bright, J., van der Walt, S.J., Brett, M., Wilson, J., Millman, K.J., Mayorov, N., Nelson, A.R.J., Jones, E., Kern, R., Larson, E., Carey, C.J., Polat, I., Feng, Y., Moore, E.W., VanderPlas, J., Laxalde, D., Perktold, J., Cimrman, R., Henriksen, I., Quintero, E.A., Harris, C.R., Archiald, A.M., Ribeiro, A.H., Pedregosa, F., van Mulbregt, P., SciPy 1.0 Contributors, 2020. Scipy 1.0: fundamental algorithms for scientific computing in Python. Nat. Methods 17, 261–272.
Ward, G.H., 1997. Processes and trends of circulation within the Corpus Christi Bay National Estuary Program study area. technical report CCBNEP-21. Texas Natural Resources Conservation Commission, Austin, TX.
Welch, B.L., 1947. The generalization of 'student's' problem when several different population variances are involved. Biometrika 34, 28–35.
Wolny, J.L., Egerton, T.A., Handy, S.M., Stutts, W.L., Smith, J.L., Whereat, E.B., Bachvaroff, T.R., Henrichs, D.W., Campbell, L., Deeds, J.R., 2020. Characterization of *Dinophysis* spp. (Dinophyceae, Dinophysiales) from the mid-Atlantic region of the United States. J. Phycol 56 (2), 404–424.
Xie, H., Lazure, P., Gentien, P., 2007. Small scale retentive structures and *Dinophysis*. J. Marine. Syst 64, 173–188.
Yasumoto, T., Oshima, Y., Yamaguchi, M., 1978. Occurrence of a new type of shellfish poisoning in the Tohoku district. Bull. Japan. Soc. Sci. Fish. 44 (11), 1249–1255.
Yasumoto, T., Murata, M., Oshima, Y., Sano, M., Matsumoto, G., Clardy, J., 1985. Diarrhetic shellfish toxins. Tetrahedron 41 (6), 1019–1025.
Yoo, Y.D., Seong, K.A., Jeong, H.J., Yih, W., Rho, J.R., Nam, S.W., Kim, H.S., 2017. Mixotrophy in the marine red-tide cryptophyte *Teleaulax amphioxeia* and ingestion and grazing impact of cryptophytes on natural populations of bacteria in Korean coastal waters. Harmful Algae 68, 105–117.
Zhang, H., Bhattacharya, D., Lin, S., 2005. Phylogeny of dinoflagellates based on mitochondrial cytochrome b and nuclear small subunit rDNA sequence comparisons. J. Phycol. 41 (2), 411–420.